AIAA 79-1708R

Evaluation of the Navigation Performance of Shipboard VTOL Landing Guidance Systems

Leonard A. McGee,* Clyde H. Paulk Jr.,* and Stanley A. Steck*
NASA Ames Research Center, Moffett Field, Calif.
and
Stanley F. Schmidt† and Antony W. Merz‡
Analytical Mechanics Associates, Inc., Mountain View, Calif.

The objective of this study was to explore the performance of a VTOL aircraft landing approach navigation system that receives 1) data from either a microwave scanning beam or a radar-transponder landing guidance system, and 2) information data-linked from an aviation facility ship. State-of-the-art low-cost-aided inertial techniques and variable gain filters were used in the assumed navigation system. Compensation for ship motion was accomplished by a landing-pad deviation vector concept that is a measure of the landing pad's deviation from its calm-sea location. The results show that the landing guidance concepts were successful in meeting all the requirements of a current navigation error specification, provided that vector magnitude of the allowable error, rather than the error in each axis, is a permissible interpretation of acceptable performance. The success of these concepts, however, is strongly dependent on the distance measuring equipment bias. In addition, the "best possible" closed-loop tracking performance achievable with the assumed point-mass VTOL aircraft guidance concept is demonstrated.

Nomenclature

a_{TC} = total acceleration command
az = azimuth angle
$D^2_{(\cdot)}$ = variance of the $(\cdot)$ position component
el = elevation angle
g = acceleration of gravity
H_A = height of landing guidance system antenna above ship's center of gravity
H_s = significant wave height
$K(\cdot,\cdot)$ = complementary filter gains
R = measured DME range
R_c = computed DME range
T_0 = modal wave period
V_{wind} = ambient wind magnitude
X,Y,Z = aircraft position components with respect to ship's landing guidance system
Z_s = ship's heave distance
θ_s = ship's pitch angle
$\sigma_{(\cdot)}$ = error standard deviation of the $(\cdot)$ measurement
$\sigma^2_{(\cdot)}$ = error variance of the $(\cdot)$ measurement
ϕ_s = ship's roll angle
ψ_s = ship's course angle

Introduction

VTOL aircraft operations from small aviation facility ships in all-weather conditions require navigation and guidance capability that will provide the necessary information for a controlled instrument approach, hover, and landing. Under the most demanding conditions, those landings must be made on a 12.2 m (40-ft) square landing pad on a ship that is underway and subject to both attitude and translational motion. To compute the position and velocity of the aircraft in an appropriate coordinate frame, the navigation system onboard the VTOL aircraft must use information provided by the ship's landing guidance system and information data-linked between the ship and the VTOL aircraft regarding the relative motion of the landing pad.

One operational automatic landing guidance system, the AN/SPN-42 (Ref. 1), is in use. This system, however, cannot provide the short-range coverage and accuracy required for VTOL operations. Systems under development such as the Marine Remote Area Approach and Landing System (MRAALS) and the civil MLS (a microwave scanning beam system with C-band distance measuring equipment) are not precise enough to provide automatic guidance to touchdown for flight operations to a small landing pad. Optical systems using lasers can provide precise measurements but lack sufficient penetration in fog or heavy rain. There are, however, promising candidate techniques under consideration that may be able to meet the required stringent navigation position and velocity accuracies at an acceptable cost and weight. The two most promising are 1) a K-band frequency-modulated/continuous wave radar-transponder (R-T) system; and 2) a Ku-band microwave scanning beam (MSB) system. The objective of this study was to examine the navigation performance of these two landing guidance systems.

For the R-T system, a transponder is located on the VTOL aircraft; aircraft position is computed by the shipboard system and data-linked to the aircraft. For the MSB system, aircraft position is measured on board the VTOL aircraft. These two systems are physically quite different in implementation, but both provide measures of VTOL aircraft range, azimuth angle, and elevation angle with respect to the ship. For this reason the two physical systems were assumed mathematically equivalent for the purpose of analysis. Henceforth, except for the discussion of physical implementation in the next section, only the performance of a single "candidate" landing guidance system with varying error characteristics will be considered.

Ship motions result in the computed aircraft position being measured in a rotating and translating coordinate system. Removal of these motion effects was accomplished through a concept that employs a landing pad deviation vector (LPDV).[2] This vector represents the nominal deviation of the landing pad from the calm sea condition. The LPDV is described in a later section.

Presented as Paper 79-1708 at the AIAA Guidance and Control Conference, Boulder, Colo., Aug. 6-8, 1979; submitted Nov. 8, 1979; revision received Dec. 5, 1980.

*Research Scientist.
†Senior Scientist. Associate Fellow AIAA.
‡Senior Analyst. Member AIAA.

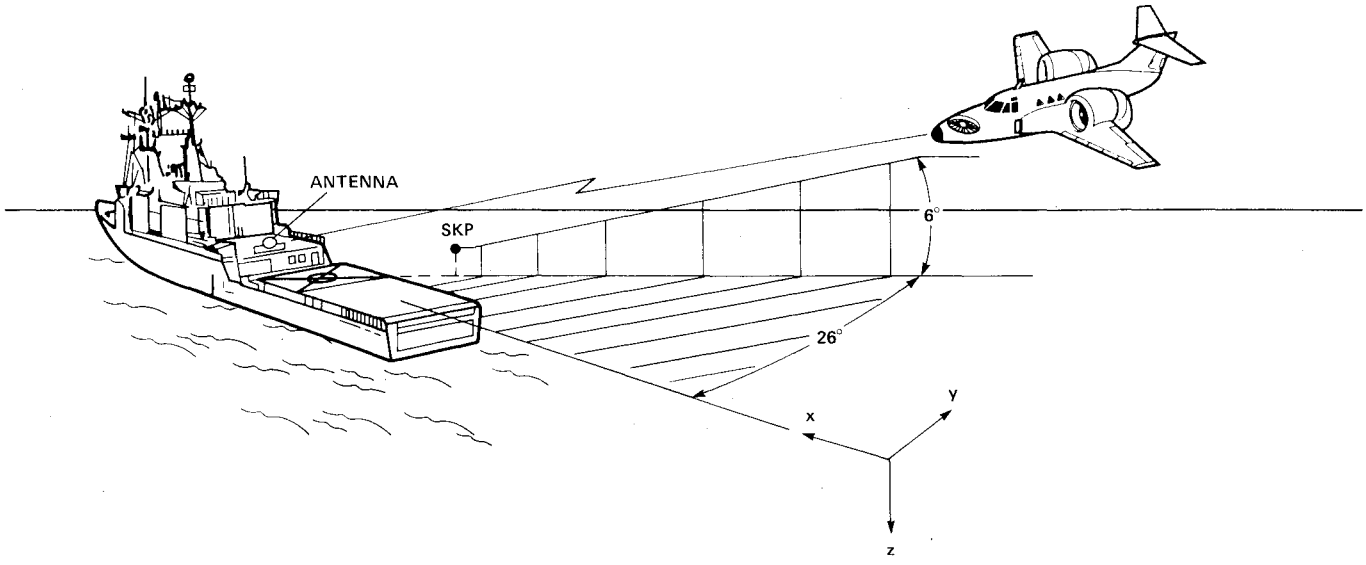

Fig. 1 General geometry for VTOL approach and landing.

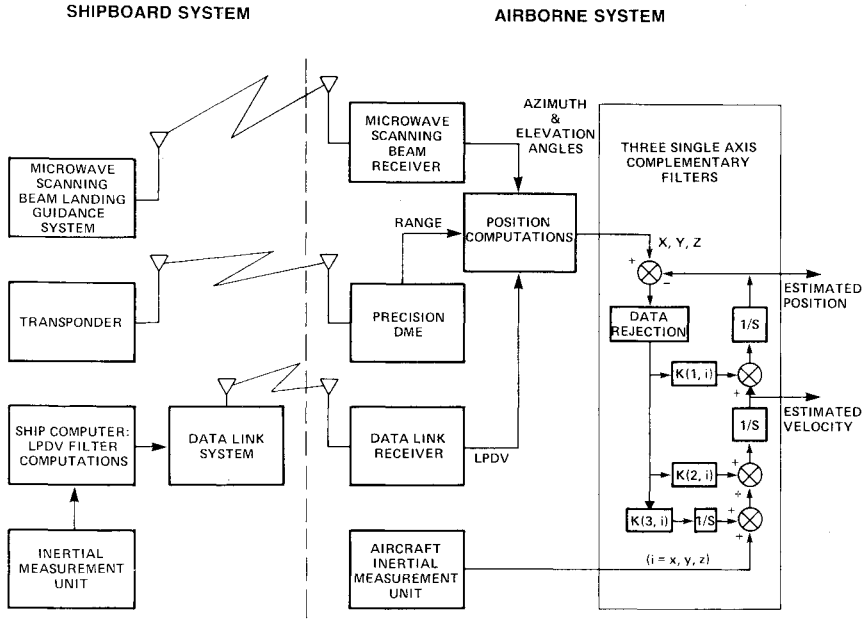

Fig. 2 Microwave scanning beam landing guidance system.

The analysis was performed using a digital simulation operating on a CDC 7600 computer. For this study, many of the error models were based on flight test experience. The aircraft navigation computer was assumed to process data from the aircraft's sensors and data from the candidate landing guidance system to compute position components with respect to the ship. After correction for ship motion, those components and measured inertial information from the aircraft system were input into complementary filters to produce estimates of the aircraft state. Those estimates were then input into a simple closed-loop guidance system, which assumes a point-mass model for the aircraft. The guidance law computed the proper commands for the aircraft to execute a constant 26 deg relative-bearing approach to the stationkeeping point (SKP) near the ship's landing pad. In addition, during the approach, the guidance law caused the aircraft to follow a reference path in the vertical plane that included intercept, descent, and flare phases ending at the SKP. The investigation of the descent from the SKP to the landing pad was beyond the scope of this study. Conclusions presented are based on comparisons of current specifications[1] with the navigation performance of the candidate landing guidance system and the effect on that performance of 1) distance-measuring equipment (DME) range errors, 2) measurement biases, and 3) sea state.

Landing Guidance Systems Concepts

The general geometry of the VTOL approach and landing problem is shown in Fig. 1. The ship is moving at a speed of 37 km/h (20 knots) along the x axis and, in addition, is undergoing motions induced by wind and sea. These attitude and translation motions are measured by a shipboard inertial measurement unit (IMU), and the required information derived from these data is data-linked to the VTOL aircraft in a north-oriented local-level (NOLL) coordinate system. The antenna location for both landing guidance systems is shown in Fig. 1. The antenna in this study was not stabilized for the ship's pitch and roll motions.

Figure 2 shows an implementation of the MSB landing guidance system in which DME range, azimuth angle, and elevation angle are measured in the airborne MSB receivers and fed to the airborne computer. The LPDV computations are done on the ship and then data-linked to the airborne computer. The airborne computer uses range, azimuth, and elevation information to compute position components that are transformed into NOLL coordinates; the NOLL coor-

dinates are then summed with the LPDV components to correct for ship motion. The airborne IMU sends aircraft acceleration components to the airborne computer, which transforms them into the NOLL coordinate system and adds the acceleration of gravity. Each aircraft position component and the respective acceleration component are fed into one of three single-axis, variable-gain, complementary filters to produce the estimated aircraft position and velocity.

The R-T landing guidance system produces comparable position and velocity estimates but by a different method. With the R-T method, the measurements are made aboard the ship. The shipboard computer uses the DME range, azimuth angle, and elevation angle to compute and transform the aircraft position components into NOLL coordinates and then corrects for ship motion using the LPDV. As is the case with the MSB system, these components are then data-linked to the airborne computer, which calculates the estimated aircraft position and velocity.

Reference Flightpath and Guidance Strategy

To investigate the tracking performance of a closed-loop guidance strategy, a single representative flightpath and velocity profile is compared with the estimated position and velocity to produce errors; the errors are then fed to a point-mass simulation of a VTOL aircraft with respresentative flightpath dynamics, as diagramed in Fig. 3.

The three-dimesional reference flightpath is shown in Fig. 1; it was chosen to be compatible with existing ship-mounted visual landing systems that include a 26 deg "lineup line." To accomplish this, the reference flightpath maintains a constant 26 deg bearing, with respect to the ship's heading, throughout the approach to the SKP. In this study, the flightpath begins at a range of 1556 m (5105 ft) from the ship. An initial level portion is flown at a constant 121.9-m (400-ft) altitude until a 6 deg glide slope is intercepted, which, in turn, intercepts a final level segment ending at the SKP. The SKP was located at a horizontal distance of 27.8 m (91.21 ft) from the landing pad along the 26 deg visual "lineup line," at an altitude of 12.2 m (40 ft) above the mean sea level, and 6.1 m (20 ft) above the landing pad.

The velocity profile along the glide slope is characterized by three segments. The upper segment is at a constant velocity of 21.3 m/s (70 ft/s) and the middle segment is at a velocity that decreases linearly with time as the aircraft decelerates at 0.1 g until the range-to-go is 9.1 m (30 ft). In the final segment, the aircraft is caused to linearly decrease its velocity as a function of range-to-go to the SKP. This results in the distance to the SKP exponentially decreasing to zero while the aircraft's velocity is reduced until it is equal to that of the ship.

As shown in Fig. 3, the guidance equations and the estimated aircraft positions and velocities from the navigation filters were combined with the reference flightpath equations and the desired velocity profile in the guidance laws to derive along-track, cross-track, and vertical position and velocity errors. Using those errors, a total acceleration command, a_{TC}, was computed for each of the three axes. Because it was assumed that the flight path control was decoupled from the attitude control and that there were no system lags such as thrust buildups, the aircraft transfer function was unity, with the result that the aircraft acceleration was equal to a_{TC}. This acceleration vector is fed to the aircraft IMU model to produce the measured acceleration used in the complementary filters. The acceleration vector is also doubly integrated to produce the aircraft position, which is differenced with the ship's position to produce the relative position required by the landing guidance system model. This model then simulates new measurements of the DME range, azimuth, and elevation angles which, in turn, are fed to the navigation filters where new estimates of the aircraft position and velocity are computed.

Navigation Computations

The navigation computations are used to produce estimates of the aircraft position and velocity components. The estimates are computed by the complementary filters; performance depends on such other factors as navigation measurement errors, aircraft IMU measurement errors, ship motion, and the LPDV. The following discussion describes the methods used to include these factors in the navigation computations.

Position and Velocity Computations

Position Algorithm

The position components (X, Y, Z) of the VTOL aircraft in landing-pad coordinates are determined from measurements of DME range, azimuth angle, and elevation angle obtained from the typical landing guidance system, using the following equations:

$$X = -R\cos(\text{el})\cos(\text{az})$$

$$Y = -R\cos(\text{el})\sin(\text{az})$$

$$Z = -R\sin(\text{el}) \qquad (1)$$

where R, az, and el are the measured DME range, azimuth, and elevation, respectively, of the VTOL aircraft.

Complementary Navigation Filters

A block diagram of a complementary filter for the x axis is also shown in Fig. 2. All three filter axes have the same general form but have different gains. The filters are described as continuous because the integrations are preformed using rectangular numerical integration. The data rate of the filters is 10/s. The characteristic equation of the filter has three roots on a circle about the origin in the complex plane. These roots have a damping ratio of 0.707. "Gain scheduling" is used to vary the natural frequency as a function of the sensitivity of the position component error to a measure of the error variance in each measurement (DME range, azimuth, and elevation). This is accomplished in the following manner. A Jacobian matrix J, which relates the sensitivity of each position component in Eq. (1) to errors in each of the measurements, is computed and transformed from the landing pad reference into the NOLL reference. This matrix is used to compute three position variances (D_x^2, D_y^2, D_z^2) as follows:

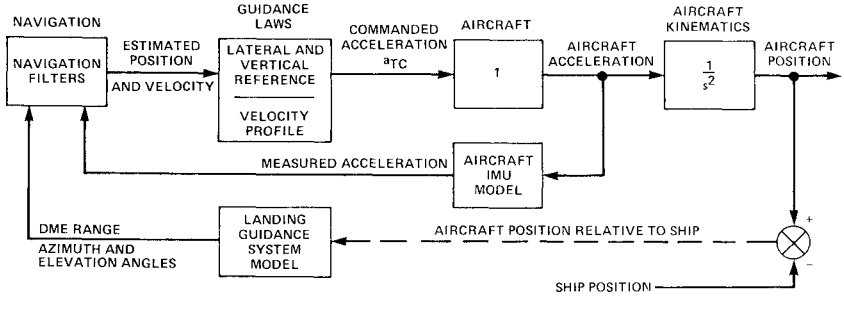

Fig. 3 Closed-loop guidance and navigation.

$$\begin{bmatrix} D_x^2 & x & x \\ x & D_y^2 & x \\ x & x & D_z^2 \end{bmatrix} = \begin{bmatrix} \\ J \\ \\ \end{bmatrix} \begin{bmatrix} \sigma_R^2 & 0 & 0 \\ 0 & \sigma_{az}^2 & 0 \\ 0 & 0 & \sigma_{el}^2 \end{bmatrix} \begin{bmatrix} \\ J \\ \\ \end{bmatrix}^T \tag{2}$$

where σ_R^2, σ_{az}^2, and σ_{el}^2 are variances that represent the combined effect of all bias and random errors in each measurement. The performance is optimized for a particular measurement error level by experimentally selecting σ_R^2, σ_{az}^2, and σ_{el}^2. The resulting D^2's in Eq. (2) represent the position error variance in each axis due to the three selected variances. The square root of these variances, $D_i\,(i=X,Y,Z)$, is used in the scheduling computations for each axis, causing the filter gains to vary inversely with the error standard deviation. As a result, the filter's response increases as the aircraft approaches the landing pad. Experience has shown that it is also necessary to restrict the dynamic range of the filter gains so that aircraft control system activity is within tolerable levels. This was accomplished by restricting the D's as follows:

$$0.1 \le 1/D_i \le 2.0 \qquad (i=X,Y,Z)$$

The filter gains are then computed as follows:

$$K(1,i)=2.414/D_i \quad K(2,i)=2.414/D_i^2 \quad K(3,i)=1.0/D_i^3 \qquad (i=X,Y,Z)$$

Figure 2 also shows a block labeled "data rejection" to indicate the location where the data rejection scheme was employed in the complementary filters to avoid processing "bad" data. Bad data occur when the error defined by the magnitude of the measured DME range minus the range computed from filter position estimates exceeds a tolerance level. The tolerance, based on experience with an MLS system, was given by

$$\text{Tolerance} = 0.006\,R_c + \sigma_R + |\text{range bias}| + 15.2 \text{ m}$$

where R_c is the computed DME range from the filter estimates. This tolerance represents the worst-case error. It includes a range-dependent term (0.6% of the computed range), the range bias, and the error standard deviation σ_R, plus a constant to allow for a period of filter dead reckoning since the last good measurement. If the data are found to be bad, the filter dead reckons until the next data sample. In this study, 2% of the simulated data for each measurement was randomly generated as bad data.

For each data run, it was necessary to initialize the complementary filters. Initialization consisted of using the position algorithm, Eq. (1), every 0.25 s to compute three position components which were transformed to NOLL, corrected for ship motion (LPDV), then saved sequentially until 20 position points (5 s of data) had been stored. A straight-line, least-squares fit was then made to each set of 20 position components to determine initial positions and velocities.

Error Models

The error models for the transmitted DME range, azimuth, and elevation angles for the candidate landing guidance system were modeled as having both random noise and fixed bias terms. The Gaussian distributed random noise terms were modeled as the output of a first-order filter having a known white noise input 1σ value and a known time constant. Parameters for four error models defining cases A, B, C, and D of the candidate system are given in Table 1. These cases represent increasing levels of both bias and random error selected to cover the spectrum of expected system DME accuracies. Case A is believed to be representative of the most accurate system achievable with current technology.

Errors in the airborne accelerometer measurements were modeled as a misalignment of the accelerometer axes, random noise, scale factor errors, and truncation errors. The three misalignment errors were each modeled as having a nominal cone angle of 0.2 deg, which was selected at the start of each case as a sample from an ensemble having a uniform density function between ± 180 deg. The random noise, also modeled as the output of a first-order filter with white noise input, had a standard deviation of 0.03 m/s^2 (0.1 ft/s^2) and a time constant of 1 s. A scale factor error of 0.1% was applied to the sum of the misaligned accelerometer outputs and the random noise. These measured accelerations were assumed to be in the form of analog voltages which were fed to digital converters. The converter was assumed to add truncation errors of 0.001 m/s^2 (0.0033 ft/s^2) in the horizontal channels and 0.0025 m/s^2 (0.008 ft/s^2) in the vertical channel.

The random error in sensing the attitude angles was modeled in the same manner as the accelerometer random noise. The standard deviation (1σ) was 1 deg and the time constant was 60 s.

The shipboard IMU was assumed to have a higher quality attitude and heading measurement system than that of the aircraft. Because the accelerometer triad, mounted near the center of the landing pad, was assumed to be better calibrated and instrumented than the airborne triad, accelerometer scale factor and truncation errors could be neglected. Therefore, the random errors in the ship attitude measurements were modeled in the same fashion as for the aircraft, except that the attitude error standard deviation was 0.1 deg and the time constant was 600 s. The accelerometer error model and the misalignment error model were identical to those of the aircraft system.

The error models presented in this section were used in conjunction with random number generators to produce the individual sample runs used in the subsequent simulation computations. The choice of error parameters was based primarily on experience with similar devices.

Ship Motion Simulation

The ship motion in this simulation is modeled after that of the DD-963 destroyer. The motions were generated using the sum-of-sinusoids model described in Ref. 3. That model assumes the seaway is long-crested, which implies that the ambient wind and waves are parallel and unidirectional. These conditions create the severest sea environment. Ship motions are generated for each of the six degrees of freedom

Table 1 Candidate system case error models

	DME range			Azimuth and elevation angles		
		Noise			Noise	
Case	Fixed bias, m (ft)	1σ, m	Time constant, s	Fixed bias, deg	1σ, deg	Time constant, s
A	0.15 (0.5)	0.15	0.1	0.1	0.1	0.1
B	0.30 (1.0)	0.30	0.1	0.1	0.1	0.1
C	0.91 (3)	0.91	0.1	0.1	0.1	0.1
D	3.05 (10)	3.05	0.1	0.1	0.1	0.1

Table 2 Ship-motion characteristics as a function of sea state

	Sea characteristics			1σ values		
Sea state	V_{wind}, knots	H_s, m	T_0, s	σ_{ϕ_s}, deg	σ_{θ_s}, deg	σ_{Z_s}, m
5	25	3.66	13.5	2.0	0.77	1.04
3	17.7	1.40	8.8	1.1	0.34	0.61
0	0	0	0	0	0	0

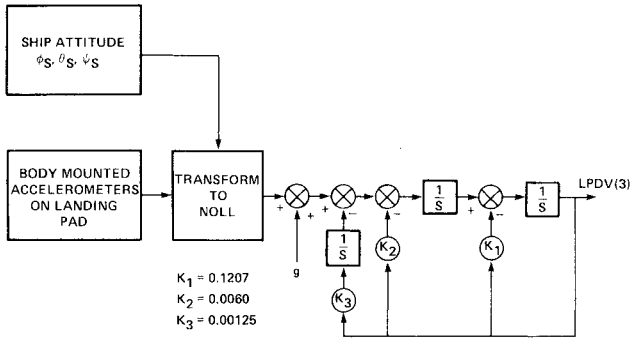

Fig. 4 LPDV vertical component filter.

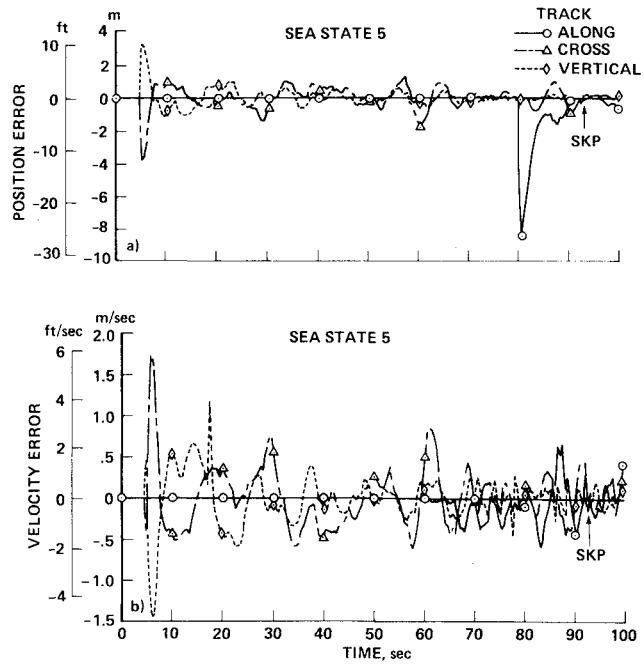

Fig. 5 Navigation errors for candidate system case B.

by summing six appropriately weighted and phased sinusoidal components. Various sea-state representations are characterized by the ambient wind magnitude V_{wind}, the significant wave height H_s, and the modal wave period T_0. For the present study, three sea-state conditions were used: 0 (smooth), 3 (moderate), and 5 (very rough). The associated sea characteristics and 1σ values of the predominant motions in the ship roll (ϕ_s), pitch (θ_s), and heave (Z_s) directions are given in Table 2.

Landing-Pad Deviation Vector (LPDV)

During the approach, the position of the aircraft, in landing-pad coordinates, is determined from the results of the position algorithm. The landing pad may be undergoing substantial angular and translational motion, however, depending on the sea state. The approach used to solve this problem was to use a landing-pad deviation vector to compute the nominal deviation of the landing pad from the calm sea condition. The LPDV has two horizontal components, LPDV(1) and LPDV(2), and a vertical component, LPDV(3). The two horizontal components are computed as follows:

$$\text{LPDV}(1) = -H_A \sin\phi_s \sin\psi_s \qquad \text{LPDV}(2) = H_A \sin\phi_s \cos\psi_s \quad (3)$$

where $H_A = 6.1$ m (20 ft). The angles ϕ_s and ψ_s are, respectively, the measured ship roll and nominal course angles referenced to north. As a result of using these simplified computations for the LPDV horizontal components, some ship-motion effects are not removed from the navigation estimates. Consequently, the aircraft's guidance system is forced to follow some of the lateral and longitudinal motions of the landing pad. Nevertheless, when contrasted with the LPDV concept first introduced in Ref. 2, which had second-order filters in each axis and a very high-quality IMU with external updating to control drift, this approach has several advantages. They are: 1) no filters or information, sensed by an expensive, high-quality, gimballed IMU, are necessary to compute the LPDV horizontal components; 2) the ship IMU can be a relatively low-cost, body-mounted accelerometer triad coupled with the ship's normal attitude and heading sensors; and 3) the ship can be permitted to execute mild turns even when the aircraft is at the SKP. The disadvantage of the approach is that there is a slight degradation in the navigation X and Y position and velocity estimates.

The vertical component of the LPDV, LPDV(3), is computed by a third-order filter to achieve a zero steady-state error, since the average vertical ship motion must be zero. Figure 4 shows that the ship's accelerometer signals are transformed into NOLL coordinates using the ship's attitude angles. Only the vertical component is retained and appropriately combined with the gravity vector "g" to become the input to the third-order filter. The characteristic equation of the filter has three roots on a circle about the origin in the complex plane. The complex roots have a damping ratio of 0.707 and a natural frequency of 0.05 rad/s.

Results

Results will be presented for candidate system cases A-D covering the spectrum of expected DME accuracies. These results show: 1) typical navigation error time histories for candidate system case B; 2) effects of fixed biases on position estimates (case D without random noise); 3) rms navigation errors for cases A-D; 4) the effect of three levels of sea state on case B; 5) a comparison of the navigation performance of case B with accuracy specifications; and 6) the tracking performance of a closed-loop guidance strategy, using a point-mass aircraft model with the case B navigation system.

The rms results were obtained by making ten Monte Carlo runs for each sea state and for cases A-D. For each run, the navigation errors were defined as the differences between the position and velocity estimates and the corresponding actual flight-path values. These errors were computed as a function of time along the reference flight path. The rms position and velocity errors for the Monte Carlo runs were then computed as a function of time. The low-frequency ship-motion effects were not sufficiently removed by the ten-sample Monte Carlo averaging process. Indeed, many more samples would be required for a good average. To achieve the effect of a large-sample rms average, a line was faired through the Monte Carlo results and used to obtain the rms data presented in the following figures and tables.

Navigation Performance

Typical Navigation Error Time Histories

Figure 5a shows the position error time histories for candidate system case B. The sea state was 5. It can be seen that at about 5 s (i.e., after the complementary filters are initialized), the position errors are at a maximum and then decrease with time. The three position components are well behaved;

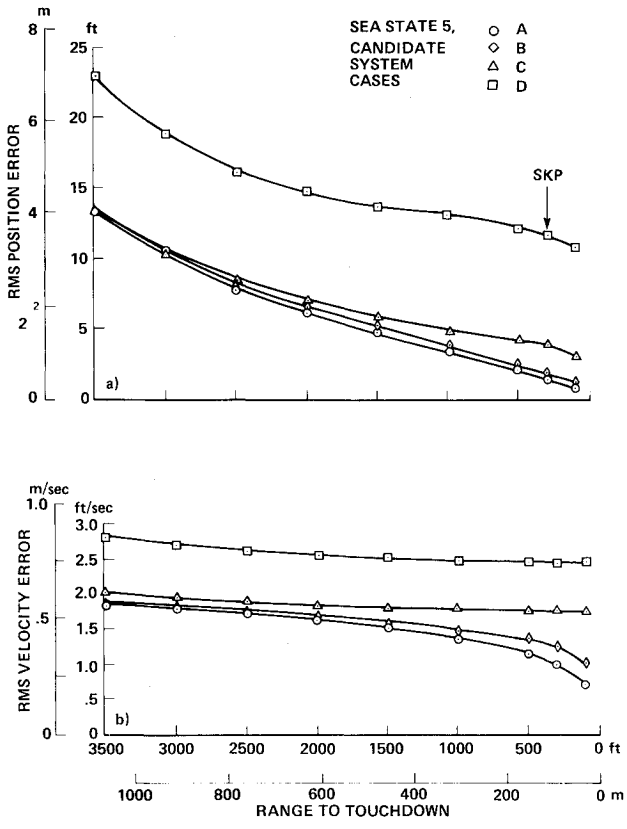

Fig. 6 Rms errors for candidate system cases A-D.

however, when compared with a similar case with no ship motion, some ship-motion effects are evident, particularly in the Y component; this is evidenced by the oscillating traces with peaks every 5-7 s. The velocity errors shown in Fig. 5b also exhibit an oscillatory behavior that is induced by ship motion. This behavior is most predominant in the Y component and persists until the final 30 s of the time history. This effect is caused by a lack of compensation for sway and yaw in the LPDV. The X velocity component also exhibits a small amplitude oscillatory behavior that decreases in amplitude by the time the SKP ($t = 92$ s) is reached. This is also due to the lack of compensation in the LPDV, except that ship surge, instead of sway and yaw, is mainly responsible. The Z velocity is the better controlled of the three components. This is due to the compensation for heave and pitch provided by the third-order filter in the vertical component of the LPDV.

RMS Navigation Error as a Function of Candidate System Case

Figure 6 shows the rms navigation position and velocity errors vs range to the landing pad for candidate system cases A-D. The sea state was 5. Range to the landing pad rather than time was chosen for the abscissa because the filter gain scheduling and bias error characteristics are nearly linear functions of range. The final 1067 m (3500 ft) of range was chosen because readability was enhanced over the area of interest. This figure shows the dependence of the navigation error on DME error. In all of the cases shown, the complementary filters performed well, reducing the rms error to approximately the DME bias error level when the aircraft was at the SKP. For the two most accurate DME's, the linear relationship between position error and range is clearly evident out to about 600 m (1968 ft), where the effect of the

Table 3 Rms navigation errors as a function of sea state

	Rms position error, m			Rms velocity error, m/s		
	Sea state			Sea state		
DME range, m (ft)	0	3	5	0	3	5
SKP—28.3 (92.8)	0.34	0.34	0.30	0.174	0.245	0.302
91.4 (300)	0.49	0.49	0.52	0.200	0.270	0.378
304.8 (1000)	0.94	1.00	1.05	0.220	0.296	0.445
457.2 (1500)	1.36	1.44	1.55	0.257	0.320	0.482
762 (2500)	2.56	2.54	2.61	0.320	0.375	0.524
1066.8 (3500)	4.08	3.90	4.08	0.390	0.448	0.561

Table 4 Comparison of rms navigation errors and specifications at key points

		Rms error, m		Error specification, m	
Range of key point, m		Component	Vector magnitude	Component	Vector magnitude
			Position		
	X	0.46		0.30	
91.4 (300)	Y	0.18	0.52	0.30	0.53
	Z	0.18		0.30	
	X	0.27		0.30	
28.3 (92.8)	Y	0.09	0.30	0.30	0.53
	Z	0.09		0.30	
			Velocity		
	X	0.17		0.30	
91.4 (300)	Y	0.31	0.38	0.30	0.53
	Z	0.12		0.30	
	X	0.15		0.30	
28.3 (92.8)	Y	0.23	0.30	0.30	0.53
	Z	0.11		0.30	

angle bias errors become important. For the two least accurate DME's, there is a nonlinear effect that is not seen when the more accurate DME's are used. This effect is due to the complementary filter gain scheduling which, because of the limited scope of this study, was only partially optimized. The dominance of angular bias errors at the larger ranges is evidenced by the upswing of all error traces at the larger ranges. This upswing is delayed by mutual cancellation of range bias and angle bias effects. As a result, the traces for the three most accurate DME's converge at a range of 1067 m (3500 ft).

The complementary filters provide an accurate estimate of the velocity, particularly near the SKP, using the two most accurate cases, A and B. This is achieved despite the relatively high sea state and the lack of direct velocity data to the complementary filters. At greater ranges, however, some improvement appears possible. Using the two least accurate cases, C and D, the velocity errors do not reduce in the vicinity of the SKP, indicating that further modification of the filter gain scheduling is warranted.

RMS Navigation Error as a Function of Sea State

The data in Table 3 were computed assuming case B of the candidate system. Case B was chosen because it is probably about the best attainable, with current technology, in a shipboard environment. Table 3 gives the rms navigation error at several ranges from the landing pad and as a function of the sea state. Allowing for some variation in the data shown, there appears to be only a slight effect, if any, on the navigation position error due to sea state.

The rms velocity errors (Table 3) show some effect of sea state. The increase in velocity error of sea state 3 over sea state 0 is about 0.07 m/s (0.23 ft/s). The increase in velocity error of sea state 5 over sea state 3 is about 0.15 m/s (0.5 ft/s), except at the SKP and at the 91.4 m (300 ft) range, where the velocity error increase is only 0.06 m/s (0.2 ft/s) and 0.09 m/s (0.3 ft/s), respectively. These errors, both in position and velocity, show that the LPDV is quite effective in removing most of the influence of sea state from the navigation estimates.

Comparison of Navigation Performance with Accuracy Specifications

The navigation accuracy specification[1] currently requires the error in each position axis to be less than 0.3 m (1 ft), and the error in each velocity axis to be less than 0.3 m/s (1 ft/s) at ranges less than 91.4 m (300 ft). For comparison with the specifications, the candidate system case B was used. Table 4 shows the individual X, Y, and Z component rms errors for both position and velocity at each of two key points: 1) 91.4 m (300 ft) range, and 2) the SKP range [28.3 m (92.8 ft)]. In addition, the vector magnitude of the errors is shown. It can be seen that the error specification for each individual axis is satisfied except at a range of 91.4 m. At that key point, the X position component exceeds the requirement by 0.16 m (0.5 ft) or 53%, and the Y velocity component exceeds its specification by 0.01 m (0.03 ft) or 3%. In each case, however, the remaining two components of error are quite small. If the vector magnitude of the allowable navigation error, rather than the error in each axis, is a permissible interpretation of acceptable performance, then the allowable error is 0.53 m (1.73 ft) in position and 0.53 m/s (1.73 ft/s) in velocity. With that assumption, the vector magnitude columns in Table 4 show that the example system would provide acceptable accuracy at both key points. It should also be noted that additional studies to optimize gain scheduling for the complementary filters should result in an improved performance that would make it possible to meet all specifications.

Closed-Loop Guidance System Performance

The tracking performance of the closed-loop point-mass VTOL aircraft guidance system using the candidate system case B is shown in Fig. 7. Figure 7 shows the position and velocity error from the reference flightpath, which, in turn, is referenced to the LPDV. These are the errors used to feed the variable-time-of-arrival guidance law computations; they are given in along-track, cross-track, and vertical-track coordinates. The position error in Fig. 7a shows two large spikes. The first, due to initialization errors, begins at 5 s. The second, beginning at 78 s, involves only the along-track coordinate which is zero (not explicitly used by the guidance system) until 78 s, when the final speed reduction is initiated as the aircraft descends to the altitude of the SKP. At that time, the large spike is the "error" or range-to-go to the SKP. The guidance system then commands a deceleration in order for the VTOL aircraft to arrive at the SKP with zero along-track velocity. The figure shows that the aircraft arrives at the SKP with along-track, cross-track, and vertical-track errors of -1.3, 0.4, and 0.1 m (4.3, 1.3, and 0.4 ft), respectively. The velocity in Fig. 7b shows, in addition to initialization errors at 5 s, a large spike in the vertical error at 17 s. This occurs as the reference 6 deg glide slope is captured. The along-track velocity error is zero (not explicitly used by the guidance system) until 60 s, when an along-track 0.1 g deceleration is initiated, followed at 78 s by the final along-track speed reduction, which, based on range-to-go from the navigation estimates, attempts to exponentially r luce the along-track error to zero. When compared to the sea-state-0 case, the effect of ship motion, particularly in the cross-track component of the velocity error, is clearly visible in this figure.

Table 5 Comparison of rms navigation and guidance errors at SKP

	Navigation errors		Guidance errors	
	Component	Vector magnitude	Component	Vector magnitude
	Rms position error, m			
X	0.27		0.66	
Y	0.09	0.30	0.10	0.67
Z	0.09		0.11	
	Rms velocity error, m/s			
$\dot{X}$	0.15		0.20	
$\dot{Y}$	0.23	0.30	0.33	0.41
$\dot{Z}$	0.11		0.12	

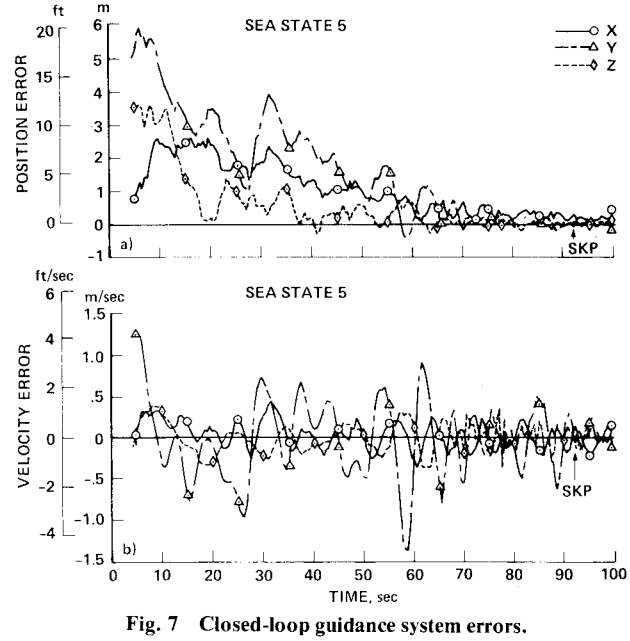

Fig. 7 Closed-loop guidance system errors.

The rms guidance and navigation errors are compared in Table 5 at the SKP because the guidance system attempts to drive the along-track error to zero only at the SKP. For these comparisons, the rms guidance errors in the along-track, cross-track, and vertical-track coordinates have been transformed into X, Y, and Z coordinates. For both the navigation and guidance errors, the vector components and their vector magnitudes are shown. The rms errors in the individual components show that the guidance errors are highly dependent on the navigation errors; that is, where larger navigation errors occur, correspondingly larger guidance errors also result. Thus, a reduction in the navigation error can be expected to reduce the guidance error. The vector magnitudes show that the position error in the navigation estimates is 0.3 m (1 ft) and the corresponding guidance error is 0.67 m (2.2 ft). In velocity, they show that the navigation error is 0.3 m/s (1 ft/s) and that the guidance error is 0.41 m/s (1.3 ft/s). Therefore, in terms of rms vector magnitude, the guidance errors exceed the navigation errors by 123% in position and 37% in velocity. The closed-loop tracking performance shown is the "best possible" that can be achieved with the assumed point-mass VTOL aircraft guidance concept, using the navigation estimates from the candidate system case B landing guidance system.

Conclusions

1) State-of-the-art inertial techniques and variable gain navigation filters were combined with a representative landing guidance system resulting in a concept that would meet the current Navy accuracy specifications for VTOL landing, providing that the vector magnitude of the allowable error, rather than the error in each axis, is a permissible interpretation of acceptable performance.

2) Range bias errors in distance-measuring equipment (DME) dominate the navigation errors near the stationkeeping point (SKP).

3) Angle bias errors of 0.1 deg have a negligible effect on navigation errors at the shorter ranges, but become dominant at larger ranges.

4) Random errors have little effect on navigation performance near the SKP with good filter gain scheduling.

5) The landing-pad deviation vector (LPDV) concept appears to be an effective low-cost method for removing most of the ship-motion effects from the navigation estimates.

6) Sea-state effects are significant only on the navigation velocity estimates.

7) The closed-loop tracking performance of the assumed point-mass VTOL aircraft may be interpreted as the "best possible" for the guidance strategy that was demonstrated.

All of the above conclusions, except 5 and 6, are also generally applicable to any aircraft operating from an airport having one of the candidate landing guidance systems installed. In this case, the LPDV computations would not be required, and the navigation performance would be that given for sea state 0 in Table 3.

References

[1] Miyashiro, S.K. and Morris, F.E., "VTOL/Helicopter Approach and Landing Guidance Sensors for Navy Ship Applications," paper presented at the Navy/NASA VSTOL Flying Qualities Workshop, Navy Postgraduate School, Monterey, Calif., April 1977.

[2] McGee, L.A., Schmidt, S.F., and Miyashiro, S.K., "Navigation Performance of the TRISCAN Concept for Shipboard VTOL Aircraft Operations," *Proceedings of the AIAA Guidance and Control Conference*, Palo Alto, Calif., Aug. 1978, pp. 363-373.

[3] Fortenbaugh, R.L., "Mathematical Models for the Aircraft Operational Environment of DD-963 Class Ships," Vought Corp., Dallas, Tex., Rept. 2-255800/8R-3500, Sept. 1978.